JACS
JOURNAL OF THE AMERICAN CHEMICAL SOCIETY

Article

pubs.acs.org/JACS

Accelerated Enzymatic Galactosylation of *N*-Acetylglucosaminolipids in Lipid Microdomains

Gavin T. Noble, Faye L. Craven, Josef Voglmeir,[†] Robert Šardzík, Sabine L. Flitsch,* and Simon J. Webb*

Manchester Interdisciplinary Biocentre and the School of Chemistry, University of Manchester, 131 Princess Street, Manchester, M1 7DN, United Kingdom

Supporting Information

ABSTRACT: A fluoro-tagged *N*-acetylglucosamine-capped glycolipid that can form lipid microdomains in fluid phospholipid bilayers has been shown to be enzymatically galactosylated by bovine $\beta(1,4)$-galactosyltransferase. MALDI MS, HPLC, and LC−MS revealed that the rate of enzymatic transformation was significantly enhanced by lipid clustering; at a 1% mol/mol loading, clustered glycolipids were galactosylated 9-fold faster than glycolipids dispersed across the bilayer surface. The transformation of the GlcNAc "glycocalyx" into a Gal(β1−4)GlcNAc "glycocalyx" relabeled these vesicles, making them susceptible to agglutination by *Erythrina cristagalli* lectin (ECL). The kinetic parameters for this transformation revealed a lower apparent K_m when the substrate lipids were clustered, which is attributed to multivalent binding to an extended substrate cleft around the active site. These observations may have important implications where soluble enzymes act on substrates embedded within cellular lipid rafts.

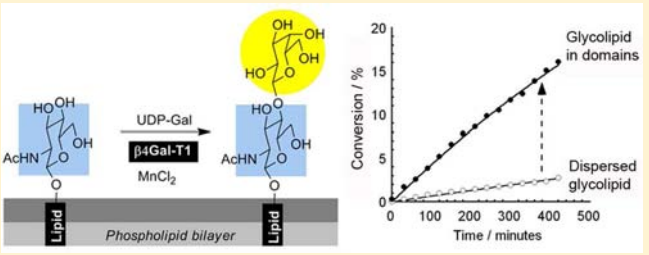

INTRODUCTION

The modification of membrane-bound substrates, such as lipoproteins or glycolipids, is a key enzymatic transformation.[1] Many enzymes involved in interfacial reactions are membrane-bound but several important transformations require soluble enzymes that only weakly associate with the membrane, such as the cytosolic sialidases.[2] Compared to soluble substrates, the enzymatic modification of membrane-bound substrates presents additional factors that can influence reactivity, including enzyme partitioning to the interface, the accessibility of the reactive moiety and inhomogeneous distribution of the substrate over the surface. In particular, the effect of inhomogeneous distribution, such as clustering into cellular lipid rafts, on substrate reactivity toward weakly membrane associating enzymes has not been well studied *in vivo* or *in vitro*.[3] This is despite lipid rafts, which are clusters of proteins, cholesterol and glycolipids[4] in the cell membrane, being identified as playing key roles in important biological events like cellular communication, trafficking and signal transduction.[5]

Molecular recognition of artificial lipids in phase separated domains has been shown to produce stronger multivalent binding to membranes[6] or induce changes in vesicle morphology.[7] However, glycolipid clustering can also introduce steric barriers to recognition, while poor glycoside presentation can decrease affinity for multivalent ligands.[8] To explore these issues, we have developed a series of fluoro-tagged model lipids able to form microdomains in fluid phospholipid bilayers.[6,9] The pyrene-perfluoroalkyl membrane anchors in these lipids allow them to form phase separated domains in solid ordered (s_o) and liquid ordered (l_o) bilayers at membrane loadings as low as 1% mol/mol, but not in liquid disordered (l_d) membranes.[9b] These l_d fluorolipid domains in l_o bilayers can be thought of simple mimics for lipid rafts, which are clusters of protein and lipid within a fluid bilayer matrix.[5b] Domain formation can be inferred from pyrenyl fluorescence emission but also visualized directly using fluorescence microscopy. The extent of phase separation can be tuned by changing the cholesterol content, as phosphatidylcholine bilayers switch from the l_d phase to the l_o phase above 25% mol/mol cholesterol.[10]

Recently we created fluoro-tagged glycolipids and showed that these compounds were able to produce saccharide-capped lipid microdomains. Vesicles with these domains were recognized and agglutinated by lectins, although no enhancement in the binding of mannosyl glycolipid microdomains to concanavalin A was observed.[11] Nonetheless, the higher affinity of multivalent oligosaccharides for lectins is well-established (the "cluster glycoside effect").[12] Analogous reactivity enhancements with enzymes have been observed for multivalent "antenna" oligosaccharides,[13] so lipid microdomains would appear to offer an excellent opportunity to assess if lateral clustering of glycolipids in membranes can affect the rate of enzymatic transformations. In particular, since the clustering of pyrene-perfluoroalkyl glycolipids can be tuned through cholesterol content, these compounds allow the same substrate to be assayed when either clustered or dispersed.

Received: March 26, 2012
Published: July 17, 2012

dx.doi.org/10.1021/ja302506t | *J. Am. Chem. Soc.* 2012, 134, 13010−13017

The soluble enzyme selected was the catalytic domain of β-(1,4)-galactosyltransferase-1 (β4Gal-T1, E.C. 2.4.1.90/38), which catalyzes the transfer of galactose (Gal) from uridine diphosphate galactose (UDP-Gal) to the 4-position of terminal *N*-acetylglucosamine (GlcNAc) in elongating oligosaccharide chains.[14,15] β4Gal-T1 is membrane-bound *in vivo*, with the catalytic and transmembrane domains linked by a flexible stem that allows the catalytic site to freely access substrates.[16] However for *in vitro* studies, soluble forms with the catalytic cytoplasmic domain cleaved from the transmembrane section are commonly used. The advantages of soluble β4Gal-T1 include well-studied kinetics in solution and wide applicability to immobilized substrates. The shallow accessible substrate binding site[17] allows it to transform substrates on solid supports, including resins,[18] nanoparticles[19] and microarrays.[20] The versatility of soluble β4Gal-T1 made it an ideal model enzyme for our studies. We therefore designed fluoro-tagged GlcNAc lipid **1** (Figure 1a), which should be capable of both forming GlcNAc domains in ordered-phase phospholipid bilayers and acting as a substrate for soluble β4Gal-T1. Recent literature suggests that multivalent or clustered substrates could be subject to two opposing effects. Substrate overcrowding can decrease reaction rates, as observed during the galactosylation of immobilized GlcNAc capped alkanethiols at loadings over 70% mol/mol.[21] Alternatively, rate increases could be possible if either secondary enzyme−substrate interactions outside the active site or statistical rebinding can occur.[22,23] These studies indicate that despite substrate-containing lipid microdomains being important multivalent substrates, their reactions with soluble enzymes are poorly understood. Herein we describe the formation of artificial GlcNAc lipid microdomains of **1** in phospholipid vesicle membranes, and studies of how this inhomogeneous substrate distribution affected the galactosylation of **1** by soluble β4Gal-T1.

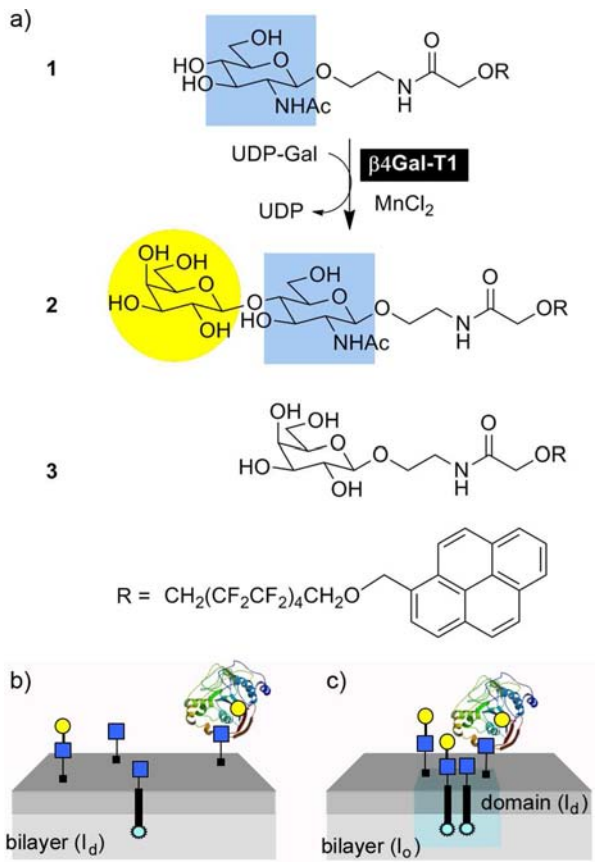

Figure 1. (a) A galactosyl group is transferred to phase separating GlcNAc lipid **1** from UDP-Gal by β4Gal-T1 to produce Gal(β(1−4)GlcNAc lipid **2**. Gal lipid **3** is a phase-separating nonsubstrate control. (b) GlcNAc lipid **1** is dispersed across the membrane in liquid disordered (l_d) bilayers like 1,2-dimyristoyl-*sn*-glycero-3-phosphocholine (DMPC) at 37 °C but (c) phase separates to form lipid microdomains (pale blue pyrenyl excimer fluorescence) in liquid ordered (l_o) membranes like DMPC/cholesterol at 37 °C.

EXPERIMENTAL SECTION

General Procedures. NMR spectra were recorded on Bruker Avance 300, DPX400 and Avance II+ 500 spectrometers at 25 °C and calibrated to the chemical shift of tetramethylsilane (δ = 0 ppm). Spectra were assigned with appropriate ^{1}H, ^{13}C, DEPT, COSY, HSQC, HMQC and HMBC NMR experiments. Chemical shifts are in ppm, coupling constants in Hertz (Hz) and multiplicities indicated with: singlet (s), doublet (d), triplet (t), double doublet (dd) and multiplet (m). ES+ mass spectra were obtained with Micromass Prospec and Micromass Platform spectrometers. IR spectra were recorded using PerkinElmer Spectrum RX I and Bruker ALPHA-P FT-IR Spectrometers. Unless otherwise specified, emission spectra were recorded at 37 °C from 360 to 600 nm (excitation 346 nm) using a Perkin-Elmer LS55 luminescence spectrometer with Julabo F25 water bath. UV−visible absorption spectra were recorded using a Jasco V-660 spectrophotometer. Fluorescence micrographs were produced using a Zeiss Axio Imager A1 fluorescence microscope fitted with a Canon Powershot G6 digital camera. MALDI measurements were made using a Bruker Daltonics Ultraflex II spectrometer. High-performance liquid chromatography (HPLC) data were obtained using an Agilent 1200 series LC system with a G1315B diode-array detector (DAD). Liquid chromatography−mass spectrometry (LC−MS) measurements were made using an Agilent 110 series LC system with an attached G1315B DAD and G1956B LC−MSD SL unit. A Phenomenex Luna C18 column (150 × 4.6 mm, 5 μm) fitted with a guard column was used for HPLC experiments. A Phenomenex Luna C18(2) column (250 × 2 mm) fitted with a guard column was used for LC−MS experiments. GUVs were electroformed using an Agilent 33210A 10 MHz function arbitrary waveform generator. (2′-Aminoethyl)-2-acetamido-3,4,5-tri-*O*-acetyl-2-deoxy-β-D-glucopyranoside[24] and 2,2,3,3,4,4,5,5,6,6,7,7,8,8,9,9-hexadecafluoro-10-(pyren-1-ylmethoxy)decyloxy)acetic acid[9b] were prepared using literature methods. Disodium UDP-Gal was purchased from Carbosynth Ltd. FITC-conjugated lectins ECL and WGA were both kind donations from GALAB Technologies. Bovine β4GalT1 was expressed in *E. coli* from bovine cDNA cloned by Dr. D. Rendic (University of Life Science, Vienna). DMPC was purchased from Avanti Polar Lipids. Other reagents were purchased from Sigma-Aldrich and used as received unless otherwise stated.

2,2,3,3,4,4,5,5,6,6,7,7,8,8,9,9-Hexadecafluoro-10-(pyren-1-ethoxy)-decyloxy-N-(2-(2-acetamido-3,4,6-tri-O-acetyl-2-deoxy-β-D-glucopyranoside)-ethyl)-acetamide (1-(OAc)$_3$). 2,2,3,3,4,4,5,5,6,6,7,7,8,8,9,9-Hexadecafluoro-10-(pyren-1-ylmethoxy)-decyloxy)-acetic acid (30 mg, 0.048 mmol), dicyclohexylcarbodiimide (DCC) (11.8 mg, 0.057 mmol, 1.2 equiv) and *N*-hydroxysuccinimide (6.6 mg, 0.057 mmol, 1.2 equiv) were dissolved in dry CH_2Cl_2 (1 mL) under N_2. The solution was left to stir for 3 h at room temperature, after which time a white precipitate had formed. The reaction mixture was filtered through cotton wool and (2′-aminoethyl)-2-acetamido-3,4,5-tri-*O*-acetyl-2-deoxy-β-D-glucopyranoside (22 mg, 0.0564 mmol, 1.18 equiv) was added in dry CH_2Cl_2 (1 mL) to the filtrate. The mixture was stirred under N_2 overnight. The mixture was filtered again and the CH_2Cl_2 was evaporated under reduced pressure. The crude mixture was partially purified using flash column chromatography (19:1 $CHCl_3$/CH_3OH on silica). Finally flash column chromatography (3:2:1 ethyl acetate/$CHCl_3$/cyclohexane on silica) yielded the product as a white solid (22.6 mg, 51%); TLC R_f 0.1 (19:1 $CHCl_3$/CH_3OH); ^{1}H NMR (400 MHz, $CDCl_3$, 25 °C): δ_H 1.94 (3H, s), 2.03 (3H, s),

dx.doi.org/10.1021/ja302506t | J. Am. Chem. Soc. 2012, 134, 13010−13017

2.04 (3H, s), 2.08 (3H, s), 3.36−3.41 (1H, m), 3.65−3.72 (3H, m), 3.84−3.92 (2H, m), 4.03 (2H, t, ^3J (H,F) = 14.0 Hz), 4.06 (2H, t, ^3J (H,F) = 13.9 Hz), 4.10−4.13 (1H, m), 4.15 (2H, s), 4.24 (1H, dd, ^3J (H,H) = 4.9, 12.3 Hz), 4.68 (1H, d, ^3J (H,H) = 8.4 Hz), 5.07 (1H, dd, ^3J (H,H) = 9.5, 9.8 Hz), 5.24 (1H, dd, ^3J (H,H) = 9.4, 10.5 Hz), 5.42 (2H, s), 5.68 (1H, d, ^3J (H,H) = 8.6 Hz), 6.80 (1H, t, ^3J (H,H) = 6.0 Hz), 8.00−8.36 (9H, m); ^{13}C NMR (100 MHz, $CDCl_3$, 25 °C): δ_c 20.9−21.0 (3 × CH_3), 23.5, 38.5, 54.6, 62.1, 67.9, 68.5, 72.0, 72.1, 72.5, 73.2, 100.4, 123.4, 124.8, 124.9, 125.3, 125.9 (2 × CH), 126.5, 127.7, 128.2, 128.5, 129.4, 129.9, 131.1, 131.5, 132.2, 168.6, 169.7−171.3 (4 × CO); MS (ES^+) m/z: 1107.2 (8%) $[M + H]^+$, 1129.3 (10%) $[M + Na]^+$; IR ν (cm^{-1}) 1022, 1095, 1169, 1260, 1465, 1668, 1732, 2853, 2923.

2,2,3,3,4,4,5,5,6,6,7,7,8,8,9,9-Hexadecafluoro-10-(pyren-1-ethoxy)-decyloxy-N-(2-(2-acetamido-2-deoxy-β-D-gluco-pyranoside)-ethyl)-acetamide (1). **1**-$(OAc)_3$ (18.3 mg, 0.0165 mmol) was dissolved in dry CH_3OH (1 mL) and 25 wt % $NaOCH_3/CH_3OH$ solution (0.1 mL) was added slowly to the stirring solution. The mixture was stirred for 0.5 h and ion-exchange resin (Amberlite IR-120) was added until the solution reached pH 7. The mixture was filtered through cotton wool and the solvent removed from the filtrate under reduced pressure to give **1** as a white solid (15.6 mg, 96%); TLC R_f 0.05 (9:1 $CHCl_3/CH_3OH$); ^{1}H NMR (400 MHz, MeOH-d_4, 25 °C): δ_H 1.88 (3H, s), 3.27−3.33 (2H, m), 3.41−3.46 (3H, m), 3.63−3.69 (3H, m), 3.86−3.90 (2H, m), 4.17 (2H, s), 4.20 (2H, t, ^3J (H,F) = 13.9 Hz), 4.23 (2H, t, ^3J (H,F) = 14.2 Hz), 4.40 (1H, d, ^3J (H,H) = 8.4 Hz), 5.41 (2H, s), 8.02−8.40 (9H, m); ^{13}C NMR (100 MHz, $CDCl_3$, 25 °C): δ_C 23.2, 40.4, 57.4, 63.0, 68.0 (t, ^3J (C,F) = 24.7 Hz), 68.9, 69.3 (t, ^3J (C,F) = 23.9 Hz), 72.3, 72.8, 74.0, 76.3, 78.2, 102.9, 124.5, 125.8, 126.0, 126.2, 126.7 (2 × CH) 127.4, 128.6, 128.7, 129.0, 129.2, 131.1, 131.3, 132.4, 132.8, 133.3, 171.5, 174.1 (CF_2 signals are weak complex multiplets); MS (ES^+) m/z: 981.3 (2%) $[M + H]^+$ 1003.3 (4%) $[M + Na]^+$; MS (MALDI) m/z: 1003.194 (100%) $[M + Na]^+$; HRMS Expected mass for $C_{39}H_{36}F_{16}N_2O_9Na$ $[M + Na]^+$ 1003.2058, found 1003.2013; IR ν (cm^{-1}) 1147, 1204, 1655, 2924, 3301−3369. UV−visible (3.6×10^4 M^{-1} cm^{-1}, 346 nm).

Preparation of GUVs and LUVs. GUVs composed of DMPC or DMPC/chol with 8.5 or 6.4% mol/mol loading of **1**, respectively, were made by slight modification of literature protocols.[25] LUVs (800 nm diameter) were created using literature protocols[9a,11] to give a final phospholipid concentration of 20 mM, synthetic lipid 0.2 mM (1% mol/mol loading). For vesicles containing higher loadings of target synthetic lipid, the synthetic lipid concentration was kept constant but the amount of phospholipid was reduced. All LUVs suspensions were freshly extruded prior to use.

Enzymatic Reaction Protocols. *General Reaction Procedure.* Vesicle suspensions containing **1** at 1.0, 8.5 or 6.4% mol/mol loading (100 μL, 200 μM **1** in 50 mM MES buffer, pH 7 at 37 °C) or PNP-GlcNAc (100 μL, 200 μM in 50 mM MES buffer, pH 7 at 37 °C), β4GalT1 solution (30 μL, estimated 11.645 μM, in MES 50 mM, 0.05% v/v TX-100, 10% v/v glycerol, pH 7 at 37 °C), UDP-Gal solution (30 μL, 10 mM in H_2O) and $MnCl_2$ solution (1 μL, 1 M in H_2O) were incubated at 37 °C.

Matrix-assisted Laser Desorption/Ionization-Time-of-Flight (MALDI-TOF MS) Analysis. Samples were spotted (1 μL) onto a polished steel plate. Sinapinic acid matrix (1 μL, 10 mg/mL in 5:3:2 $MeOH/H_2O/CH_3CN$) was spotted into the sample, mixed and allowed to dry. The plate was mounted on a transponder target frame and measurements made using a reflector positive mode.

Monitoring Reaction by LC−MS. Enzymatic reactions were performed as outlined in the general β4GalT1 reaction procedure and analyzed using LC−MS: 5 μL injects were performed on a 30 min gradient of 50:50 $CH_3CN:H_2O$ (+0.1% TFA) to 100% CH_3CN (+0.1% TFA) with a flow rate of 0.5 mL/min. The HPLC DAD module was set to detect the pyrenyl UV−visible absorption from **1** and **2** at 346 nm and the MS detector set to detect m/z 1003 (**1** + Na^+) and 1165 (**2** + Na^+). An LC peak at 14.5 min corresponded to the mass of **2**, and a LC peak at 16.5 min corresponded to the mass of **1**.

Monitoring Vesicle Reactions by HPLC. Injects (5 μL) were performed on a 30 min gradient of 50:50 THF:H_2O (+0.1% TFA) to 100% THF (+0.1% TFA) with a flow rate of 0.5 mL/min. The HPLC DAD module was set to detect the pyrenyl UV−visible absorption at 346 nm. Percent conversions were determined using the ratio of product peak area to the combined product and starting material area.

"Mixed Microdomains" β4GalT1 Reactions. DMPC/chol LUVs with a 1:9 ratio of **1**:**3** were synthesized by extrusion (0.7% mol/mol lipid **1** and 6.5% mol/mol lipid **3**: 20 mM total lipid, 140 μM **1**, 1.3 mM **3**, 50 mM MES, pH 7 at 37 °C). Enzymatic reactions were performed as previously and analyzed using HPLC: 5 μL injects were performed on a 30 min gradient of 50:50 CH_3CN/H_2O (+0.1% FA) to 100% CH_3CN (+0.1% FA) with a flow rate of 0.5 mL/min. The HPLC DAD module was set to detect the pyrenyl UV−visible absorption at 346 nm.

K_m and V_{max} Determination. β4GalT1-catalyzed reactions were performed with varying concentrations of **1** in vesicles (loading 1% mol/mol **1** in DMPC or DMPC/chol, 8.5% mol/mol **1** in DMPC, 30−250 μM **1** and 3−25 mM total lipid). Vesicle solution (16.7 μL in 50 mM MES buffer, pH 7 at 37 °C) was mixed with UDP-Gal solution (5 μL, 10 mM in H_2O), $MnCl_2$ solution (0.17 μL, 1 M in H_2O) and β4GalT1 solution (5 μL, estimated 11.6 μM, in MES 50 mM, 0.05% v/v TX-100, 10% v/v glycerol, pH 7 at 37 °C), then incubated at 37 °C. HPLC analysis was performed on aliquots (5 μL) of the samples every 30 min using the HPLC method described above. The concentration of **2** formed was determined by calculating the ratio of product peak areas to the combined product and starting material area, then multiplying it by the total glycolipid concentration (18.6−155 μM **1** + **2**). The initial rate of product formation (V) was then determined by plotting the concentration of product **2** formed against time. The values of V for each concentration (3×) were averaged and plotted against concentration of **1**. Apparent K_m and V_{max} values were determined using Origin software to curve-fit the Michaelis−Menten plot using a single-site (n = 1) nonlinear Hill fit.

RESULTS AND DISCUSSION

Lipid Microdomain Formation by 1. The syntheses of lipids **1** and **3** were performed convergently from a perfluoroalkyl-pyrene membrane anchor according literature methods.[9a] As well as allowing the direct visualization of **1** in vesicles by fluorescence microscopy, the pyrenyl fluorophore also forms excited dimers (excimers) at high local concentrations. The ratio of excimer (460 nm) to monomer (395 nm) fluorescence emission (the E/M ratio) is directly indicative of the local concentration of pyrene containing moieties and the rate of collision between them,[26] so increases in the E/M ratio indicate the formation of regions of high pyrenyl concentration.

Lipid **1** was incorporated into large unilamellar phospholipid vesicles (LUVs, 800 nm diameter) with two different compositions, dimyristoyl phosphatidylcholine only (DMPC) and a 1:1 mix of DMPC and cholesterol (DMPC/chol). These compositions were chosen because at 37 °C these bilayers are in fluid l_d, and l_o phases respectively; **1** should mix with the l_d phase but phase separate from the l_o phase.[9b] Vesicles were formed *via* repeated extrusion of a buffered aqueous suspension of lipid **1** and the desired phospholipid mixture through 800 nm polycarbonate membranes above the bilayer melting temperature (T_m). To alter the membrane loading of **1**, the phospholipid concentration was changed but the bulk concentration of **1** maintained at ∼0.12 mM. The maximum incorporation of **1** in each bilayer composition was determined using UV−visible spectroscopy, and was found to be 8.5% mol/mol **1** in DMPC and 6.4% **1** in DMPC/chol. The exchange of lipid **1** between the inner and outer leaflets (flip-flop)[9a,11] had a half-life of 60 min in DMPC and 240 min in DMPC/chol, indicating both a degree of translational freedom for the lipid in

these fluid membranes and that substrate in the inner leaflet of the vesicles would only be available during extended reaction times (>5 h).

The fluorescence emission spectra of these LUV suspensions were recorded at 37 °C, which showed that lipid **1** in DMPC/chol (1:1 mol ratio) bilayers formed domains at both 1% mol/mol (E/M = 1.5 ± 0.1) and 6.4% mol/mol (E/M = 3.5 ± 0.6). In DMPC, a much lower E/M value (E/M = 0.15 ± 0.03) at 1% mol/mol suggested no phase separation of **1**. However at 8.5% mol/mol in DMPC, lipid **1** was more crowded in the membrane and gave a higher E/M value (E/M = 1.5 ± 0.4) due to a higher rate of interpyrene collision. To visualize the membrane domains, electroformed giant unilamellar vesicles (GUVs) composed of either DMPC or DMPC/chol (1:1) with 8.5 or 6.4% mol/mol loading of **1** respectively were imaged using *epi*-fluorescence microscopy. In GUVs composed of DMPC, no large phase separated patches were observed and only weak uniform excimer emission could be observed (evenly distributed pale blue fluorescence, Figure 2a). However in DMPC/chol GUVs, domains were clearly observed (Figure 2b) with diameters up to 50 μm.

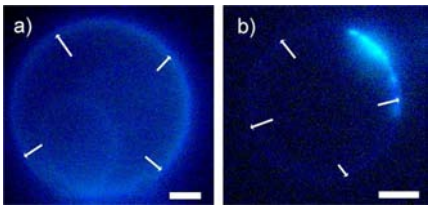

Figure 2. *Epi*-fluorescence microscopy of giant unilamellar vesicles (GUVs) (a) 8.5% mol/mol **1** in DMPC, (b) 6.4% mol/mol **1** in DMPC/chol (1:1 mol ratio). Scale bar = 20 μm. The outlines of the GUV membranes are indicated by arrows.

Enzymatic Modification of GlcNAc-lipid 1 Embedded in Vesicles. After purification of truncated His-tagged β4Gal-T1, the enzyme was obtained as a solution in 2-(*N*-morpholino)ethanesulfonic acid buffer (MES, 50 mM, pH 7) with 10% v/v glycerol and 0.05% v/v Triton X-100 (TX-100, 0.86 mM, a TX-100/phospholipid ratio of 1:10). This low concentration of TX-100 did not permeabilize the vesicle membranes but maintained enzyme stability.[27] To ascertain the strength of any enzyme/membrane interaction in the absence of substrate, DMPC vesicles were added to FITC-labeled β4Gal-T1. A decrease in fluorescence was observed, which could be due to an increase in self-quenching after localization at vesicle membranes[28] or a change in environment around the fluorophore during membrane association.[29] Analysis of the binding curve gave $K \approx 2700$ M^{-1}, confirming that soluble β4Gal-T1 only weakly associated with DMPC bilayers.

The transformation of **1** into **2** by β4Gal-T1 was assayed by HPLC, LC−MS and MALDI-MS. The enzyme (2.16 μM), UDP-Gal (1.86 mM, K_m = 93 μM[30]) and $MnCl_2$ (6.21 mM, K_m = 0.34 mM[31]) were mixed with DMPC or DMPC/chol vesicles (12.4 mM total lipid) doped with 1% mol/mol lipid **1**. In both these cases the total bulk concentration of **1** was 0.124 mM. For the higher loadings of **1** (8.5% mol/mol **1** in DMPC and 6.4% mol/mol **1** in DMPC/chol) the total bulk concentrations of **1** were 0.11 mM and 0.08 mM respectively. After 24 h, analysis of the samples by MALDI-ToF MS revealed partial conversion of the GlcNAc headgroups of lipid **1** (Na^+ adduct of **1** at *m*/*z* 1003) to Gal(β1−4)GlcNAc headgroups in the product **2** (Na^+ adduct of **2** at *m*/*z* 1165, Figure 3b). The E/M ratios of the DMPC/chol vesicles changed little after the reaction,

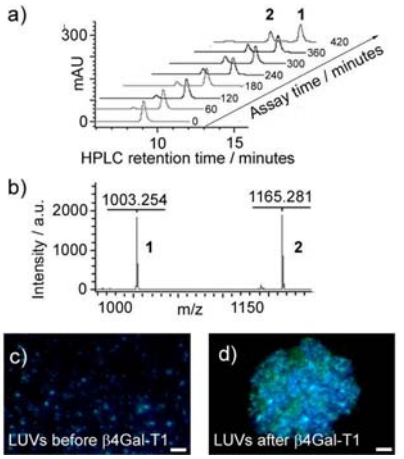

Figure 3. (a) HPLC traces showing the conversion of **1** to **2** over time (absorbance at 346 nm) (b) MS data showing the clean conversion of **1** (*m*/*z* 1003.254) to **2** (*m*/*z* 1165.281) by β4Gal-T1. (c, d) *Epi*-fluorescence micrographs of DMPC/chol LUVs (800 nm) with 6.4% mol/mol **1**, mixed with fluorescein labeled *Erythrina cristagalli* lectin (FITC-ECL). Images show (c) dispersed vesicles before and (d) agglutinated vesicles after treatment with β4Gal-T1/UDP-Gal. Images overlay fluorescein and pyrenyl emission. Scale bar 20 μm.

suggesting that enzymatically transformed lipids were still within phase separated domains. Both **1** and **2** could be clearly resolved on a reverse phase C18 column without prior purification of the reaction mixtures (Figure 3a), which allowed direct monitoring of the conversion of **1** to **2**. The samples were analyzed by HPLC every 30 min for 8 h; peaks due to **1** and **2** showed the distinctive absorption spectrum of the pyrenyl group in **1** and **2** (λ_{max} = 346 nm). As expected, the retention time of **2** was shorter than **1** and LC−MS correlated these peaks to the corresponding lipid masses.

The enzymatic transformation of lipid **1** into lipid **2** was confirmed by lectin-mediated vesicle agglutination. Fluorescein isothiocyanate conjugated wheat germ agglutinin (FITC-WGA) and FITC-conjugated *Erythrina cristagalli* lectin (FITC-ECL) are specific for terminal GlcNAc and Gal(β1−4)GlcNAc residues respectively.[32] Prior to transformation by β4Gal-T1, DMPC/chol vesicles containing 6.4% mol/mol **1** were agglutinated by WGA but not ECL (Figure 3c). After treatment with β4Gal-T1/UDP-Gal these DMPC/chol vesicles were aggregated by both WGA and ECL (Figure 3d) as these "rebranded" vesicles now expose both GlcNAc (from unreacted **1**) and Gal(β1−4)GlcNAc (from **2**) in their artificial "glycocalyx".

Integration of the absorption bands from **1** and **2** respectively (pyrenyl group) gave the extent of product formation, which was plotted against time (Figure 4c,d) for each of the lipid compositions. In each case, only lipid **1** in the outer leaflet was initially available to the enzyme (Figure 4a,b). This analysis revealed a 9-fold increase in the initial conversion rate of **1** into **2** by β4Gal-T1 when lipid **1** was phase-separated in DMPC/chol vesicles at 1% mol/mol loading (E/M = 1.5) compared to dispersed **1** in DMPC vesicles at the same loading (E/M = 0.15) (Figure 4c). After 24 h the conversion levels for **1** into **2** were 14% for **1** in DMPC and 37% for **1** in DMPC/chol. The increase in rate occurred despite both systems having the same

dx.doi.org/10.1021/ja302506t | *J. Am. Chem. Soc.* 2012, 134, 13010−13017

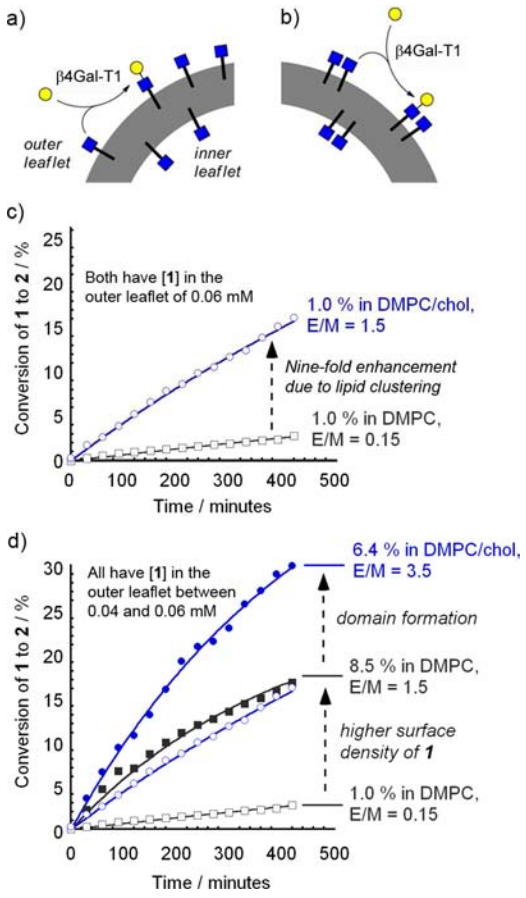

Figure 4. (a,b) Schemes showing the conversion of vesicle-bound **1** to **2** by β4Gal-T1/UDP-Gal when **1** is (a) dispersed or (b) clustered. (c,d) Conversion rates for: 1% mol/mol **1** in DMPC vesicles (□); 1% mol/mol **1** in DMPC/chol (blue ○); 8.5% mol/mol **1** in DMPC (■); 6.4% mol/mol **1** in DMPC/chol (blue ●). The extent of clustering is indicated by the E/M values at 37 °C in each case. First order curve fits are shown.

bulk concentration of **1** (0.12 mM; 0.06 mM in each bilayer leaflet). Furthermore, at a higher loading of **1** in DMPC (8.5% mol/mol), HPLC analysis showed a higher galactosylation rate compared to the corresponding 1% mol/mol loading (Figure 4d). This increase occurred despite slightly lower bulk concentrations of **1** (0.11 mM rather than 0.12 mM), suggesting that cholesterol is not required to observe this rate acceleration and higher lipid proximity causes the increase in enzymatic reaction rate.[33] Nonetheless domain formation gives a further enhancement even at these high loadings, with a small 2-fold increase in reaction rate for 6.4% **1** in DMPC/chol compared to 8.5% **1** in DMPC, which mirrors the difference in the E/M values (2-fold). Nonetheless the rate for vesicle-bound **1** was always slower than for soluble acceptor substrate *p*-nitrophenyl-GlcNAc (PNP-GlcNAc); PNP-GlcNAc was initially enzymatically transformed around 20-fold faster than **1** in DMPC/chol vesicles at 1% mol/mol, reaching 40% conversion after 60 min under the same reaction conditions.

Quantifying the Effect of Glycolipid Domain Formation on Enzyme Activity. To better understand the effect of inhomogeneous substrate distribution on enzymatic activity, kinetic assays were performed with β4Gal-T1/UDP-Gal and DMPC or DMPC/chol vesicles containing 1% mol/mol of **1**. Enzymatic assays on lipid substrates bound in vesicle membranes afford analytical advantages over other methods of supporting lipid substrates, for example, vesicles give suspensions where the substrate can be used in excess over the enzyme.[34] The initial rate of reaction was measured as a function of the concentration of GlcNAc substrate (PNP-GlcNAc[35a] or **1** embedded in vesicles). The concentration of the donor UDP-Gal was held at 1.86 mM, 20-fold higher than the literature value of K_m for UDP-Gal (93 μM); similarly $[Mn^{2+}]$ = 6.2 mM, above the concentration for maximal activity.[31] These concentrations should keep the enzyme saturated with cosubstrate and cofactor, and should produce apparent Michaelis−Menten kinetics for a one-substrate enzyme. Furthermore, as flip-flop of lipid **1** occurs with $t_{1/2}$ > 60 min, only **1** in the outer leaflet of the vesicle is available to react with the β4Gal-T1/UDP-Gal complex within the initial rate time frame.

These assays revealed that even at the highest concentrations of phospholipid compatible with HPLC analysis (up to 25 mM, [**1**] = 0.25 mM), the concentration of available lipid **1** in DMPC vesicles was still significantly below the K_m. Nonlinear regression analysis of the data using Michaelis−Menten models gave an estimated K_m > 0.5 mM and a k_{cat} value of ~2 × 10^{-3} s^{-1} (Table 1). In contrast, lipid **1** in DMPC/chol vesicles gave a much lower K_m = 90 ± 5 μM, and k_{cat} of (1.9 ± 0.1) × 10^{-3} s^{-1}. These data show a clear >5-fold improvement in apparent K_m when **1** is in domains compared to **1** dispersed over the vesicle membrane, implying improved substrate binding may accelerate the transformation of phase-separated **1** by β4Gal-T1. In addition, K_m for lipid **1** in DMPC or DMPC/chol bilayers was less than for GlcNAc in solution, where literature studies give K_m between 1 and 11 mM.[13,35] This improvement in apparent K_m suggests the phospholipid bilayer may also interact directly with the enzyme,[36] which is consistent with our observation of a weak interaction with DMPC bilayers (K_d ≈ 0.4 mM).

Table 1. Calculated Values of K_m and V_{max} for the β4Gal-T1 Catalyzed Galactosylation of 1 in DMPC and DMPC/chol Vesicles at 1% mol/mol

	GlcNAc-containing substrate	
substrate/reaction medium	K_m/mM	$k_{cat}/\times10^{-3}$ s^{-1}
GlcNAc/Buffer[a]	1−11	40−1000
Dispersed lipid **1**/Bilayer	>0.5	~2
Lipid **1** in domains/Bilayer	0.090 ± 0.005	1.9 ± 0.1

[a]Taken from Qasba et al.[35] and Pâquet et al.[13]

The k_{cat} values for **1** in membranes are significantly lower compared to solution phase GlcNAc, where literature studies give k_{cat} values between 0.04 and 1 s^{-1}.[13,35] The decrease in k_{cat} for the membrane-bound substrate **1** is consistent with the observations of Ohno et al., who compared galactose oxidase activity on analogous substrates in solution and membrane phases.[37] They ascribed a decrease in V_{max} to restricted motion of the enzyme when operating on membrane-embedded substrate. However the k_{cat} values for dispersed and phase-separated **1** appear to be similar, which implies that boundary effects, where lipids at the interface between coexisting phases are more reactive, may not be a significant contribution to the faster transformation of phase-separated **1** by β4Gal-T1/UDP-Gal.[3b,38]

It was not clear if the improvement in apparent K_m for **1** in DMPC/chol was intrinsic to domain formation, for example, **1** becomes more accessible, or whether bringing substrate

molecules into proximity improves the affinity of the enzyme for **1**. To discriminate between these possibilities, two control experiments were carried out.

"Mixed microdomains" composed of 0.7% mol/mol of **1** and 6.5% mol/mol of a nonsubstrate galactose analogue **3** were created in DMPC/chol vesicles ([**1**] in outer leaflet = 0.04 mM).[11] These vesicles exhibited phase separation (E/M = 3.8 ± 0.4) comparable to DMPC/chol vesicles with 6.4% mol/mol **1** (E/M = 3.5) and were subjected to the same enzymatic reaction conditions. HPLC analysis showed that in these mixed domains the initial rate for the enzymatic transformation of **1** into **2** was three times slower than that observed at 6.4% mol/mol **1** (also with [**1**] in outer leaflet = 0.04 mM). This observation suggests locating **1** in microdomains in the membrane is not sufficient to accelerate the enzymatic transformation, and the identity of the surrounding headgroups in the domains is crucial.

Furthermore, if substrate proximity rather than the domain structure is the origin of the lower K_m, then this should be revealed by comparing vesicles displaying similar E/M values but with **1** either in domains or dispersed. A good comparison is a loading of 8.5% mol/mol **1** in DMPC vesicles, which gives the same E/M as DMPC/chol vesicles with 1.0% mol/mol **1** (Figure 4d) but without observable microdomains (Figure 2a). Measurement of the initial rates for DMPC vesicles with 8.5% mol/mol **1** gave $K_m = 65 \pm 15$ μM. This value is comparable to that observed for DMPC/chol vesicles with 1% mol/mol **1** (K_m = 90 μM) and much less than for DMPC vesicles at 1% mol/mol **1** (K_m > 0.5 mM). These observations suggest that the domains lower K_m by providing regions of high substrate density rather than by producing changes in membrane structure.

Molecular Interpretation of the Effect of Domain Formation. Several models could explain an improvement in K_m for a soluble enzyme acting on a microdomain (Figure 5a–c).

As found for phospholipase A2 (PLA_2), lipid microdomains could provide phase boundary edges where the GlcNAc headgroups on **1** are more accessible to the enzyme. PLA_2 follows a "scooting" or "quasi-scooting" mechanism where dissociation from the membrane is much slower than reaction at the interface,[39] and has been studied hydrolyzing phase-separated membranes. These studies suggested that phospholipid hydrolysis is fastest at the domain boundaries[40] where lipid fluctuations and lateral compressibility are greatest.[3b] However, unlike PLA_2, β4Gal-T1 does not associate strongly with membranes (perhaps following a "hopping" mechanism where the enzyme rapidly exchanges between vesicles[41]) and the factors believed to enhance PLA_2 reactivity at the domain boundary, like greater ease of enzyme insertion into the membrane, would not be expected to play a significant role.

Alternatively a "hopping" mechanism with a higher rate of enzyme rebinding to surface patches of high substrate density ("statistical rebinding") should increase the rate at which a soluble enzyme associates with domains and thereby also lower K_m. Yet our recent studies of concanavalin A binding to a mannose analogue of **1** did not reveal any enhancement in affinity due to lipid clustering,[11] implying that statistical rebinding to perfluoro glycolipid domains is a minor effect and rebinding of β4Gal-T1/UDP-Gal to domains of **1** is unlikely to provide a significant improvement in apparent K_m.

If significant, both statistical rebinding and access to domain boundaries should influence the rate other soluble enzymes transform clustered substrate lipids. However preliminary studies with *T. cruzi* trans-sialidase have revealed no enhancement of trans-sialidation rates upon glycolipid domain formation,[42] implying that particular enzyme structural features may be responsible. "Substrate oligomers" are known to be better substrates for β4Gal-T1, which has much higher activity with some oligosaccharides, such as chitobiose (GlcNAc(β1–4)GlcNAc) and glycoprotein *N*-glycan sequence analogues.[13,35b,43] Furthermore it is thought that membrane-bound β4Gal-T1 on the surface of sperm acts as a GlcNAc-recognizing lectin.[15] Structural determinations have revealed that UDP-Gal binding induces a conformational change in the β4Gal-T1 enzyme that opens up an extended oligosaccharide binding site (Figure 5d).[17] The opening up of this extended binding site gives enhanced conversion rates (V_{max}) and binding (K_m) of oligosaccharides, like chitobiose, chitotriose and short artificial "antenna" sequences, compared to monomeric GlcNAc. Furthermore certain types of oligosaccharide linkages, like GlcNAc(β1–2)Man(α1–6)Man, dock into the active site better than others.[35b] We suggest that clustering GlcNAc lipids into microdomains produces regions of high GlcNAc density able to interact with the extended binding cleft of the β4Gal-T1/UDP-Gal complex and produce the enhancement in K_m. The observation that the same enhancement is not observed when the headgroup surrounding lipid **1** is galactosylated is consistent with studies by Pâquet et al., who found that GlcNAc/GlcNAc "antenna" oligosaccharides had lower K_m (and higher k_{cat} values) for β4Gal-T1 than Gal/GlcNAc analogues.[13]

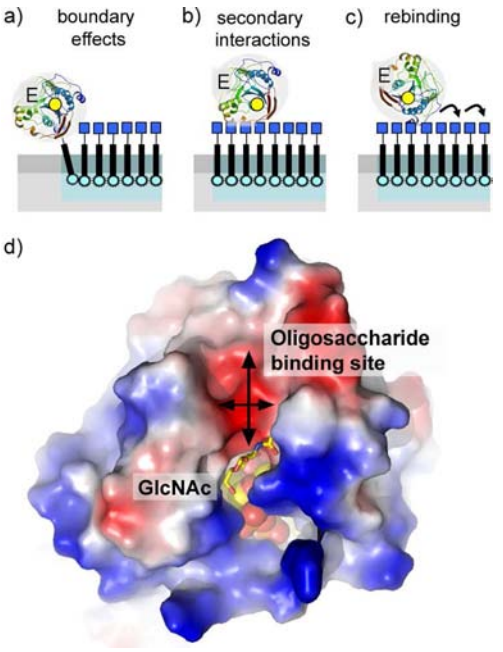

Figure 5. Simplified scheme for reaction of UDP-Gal/β4Gal-T1 (E) with a GlcNAc lipid **1** domain that illustrates possible contributions to lower K_m values: (a) preferential binding to the domain boundary; (b) secondary substrate interactions with the enzyme; (c) statistical rebinding to the domain; (d) top view of the oligosaccharide binding site edge in the UDP-Gal/β4Gal-T1 complex where the GlcNAc binding site and the extended sugar binding site can be seen (10 × 16 Å). Recreated with permission from Ramakrishnan, B.; Balaji, P.V.; Qasba P.K. *J. Mol. Biol.* **2002**, *318*, 491.

CONCLUSIONS

Clustering *N*-acetylglucolipid **1** into phase-separated domains enhanced the enzymatic transformation of this lipid by a soluble glycosyltransferase, truncated β4Gal-T1. This enhancement depended not only on the formation of domains but also on the identity of the surrounding glycolipids in the domain; mixed microdomains containing both *N*-acetylglucolipids and galactolipids did not produce the same enhancement. Detailed kinetic analysis showed that the formation of lipid microdomains with *N*-acetylglucolipids improved K_m for UDP-Gal/β4Gal-T1. Enhanced access to domain boundaries, statistical rebinding to domains and/or binding of multiple GlcNAc headgroups into a cleft on UDP-Gal/β4Gal-T1 could all explain the lower K_m for **1** in domains, but the latter explanation is the most consistent with all observations.

The observation that laterally inhomogeneous glycolipid distribution can accelerate the rate at which a soluble enzyme transforms a glycolipid may have wider implications. Many glycosyltransferases have extended binding pockets for polysaccharide substrates[45] or are processive enzymes with multiple binding subsites;[46] such enzymes could also make multivalent links to regions of high substrate density on surfaces. Given lipid rafts in cell membranes have high glycolipid densities, they could act as focal points for the action of exogenous enzymes, and indeed influenza virus sialidase is known to associate with lipid rafts.[47] In an effort to uncover these broader implications of our observations, further investigations are ongoing using other lipid substrate/soluble enzyme combinations.

ASSOCIATED CONTENT

Supporting Information

Spectra and critical aggregation concentration of lipid **1**; procedures for LUV and GUV formation; measurements of loadings and flip-flop rates; lectin aggregation of vesicles; conditions and representative MALDI-MS, LC−MS and HPLC traces for enzymatic reactions; nonlinear regression analysis of enzymatic reaction kinetics. This material is available free of charge via the Internet at http://pubs.acs.org.

AUTHOR INFORMATION

Corresponding Author

s.webb@manchester.ac.uk

Present Address

[†]Laboratory of Carbohydrate Sciences, College of Food Science and Technology, Nanjing Agricultural University, 1 Weigang, Nanjing 210095, China.

Notes

The authors declare no competing financial interest.

ACKNOWLEDGMENTS

We thank the BBSRC for providing studentship funding for F.C. and G.T.N., Prof. Nicholas H. Williams (University of Sheffield) for helpful discussions and Dr Steve Prince (MIB, University of Manchester) for providing Figure 5d.

REFERENCES

(1) Forneris, F.; Mattevi, A. *Science* **2008**, *321*, 213−216.
(2) Chavas, L. M. G.; Tringali, C.; Fusi, P.; Venerando, B.; Tettamanti, G.; Kato, R.; Monti, E.; Wakatsuki, S. *J. Biol. Chem.* **2005**, *280*, 469−475.
(3) (a) Feigenson, G. W. *Nat. Chem. Biol* **2006**, *2*, 560−563. The strongly membrane-associating enzyme phospholipase A2 (PLA_2) has been well studied. See: (b) Gudmand, M.; Rocha, S.; Hatzakis, N. S.; Peneva, K.; Mullen, K.; Stamou, D.; Uji-l, H.; Hofkens, J.; Bjoernholm, T.; Heimburg, T. *Biophys. J.* **2010**, *98*, 1873−1882.
(4) Paulick, M. G.; Bertozzi, C. R. *Biochemistry* **2008**, *47*, 6991−7000.
(5) (a) Jacobson, K.; Mouritsen, O. G.; Anderson, R. G. W. *Nat. Cell Biol.* **2007**, *9*, 7−14. (b) Lingwood, D.; Simons, K. *Science* **2010**, *327*, 46−50.
(6) Mart, R. J.; Liem, K. P.; Wang, X.; Webb, S. J. *J. Am. Chem. Soc.* **2006**, *128*, 14462−14463.
(7) Stachowiak, J. C.; Hayden, C. C.; Sasaki, D. Y. *Proc. Natl. Acad. Sci. U.S.A.* **2010**, *107*, 7781−7786.
(8) Jung, H.; Robison, A. D.; Cremer, P. S. *J. Struct. Biol.* **2009**, *168*, 90−94.
(9) (a) Liem, K. P.; Noble, G. T.; Flitsch, S. L.; Webb, S. J. *Faraday Discuss.* **2010**, *145*, 219−233. (b) Webb, S. J.; Greenaway, K.; Bayati, M.; Trembleau, L. *Org. Biomol. Chem.* **2006**, *4*, 2399−2407.
(10) Almeida, P. F. F.; Vaz, W. L. C.; Thompson, T. E. *Biochemistry* **1992**, *31*, 6739−6747.
(11) Noble, G. T.; Liem, K. P.; Flitsch, S. L.; Webb, S. J. *Org. Biomol. Chem.* **2009**, *7*, 5245−5254.
(12) (a) Lundquist, J. J.; Toone, E. J. *Chem. Rev.* **2002**, *102*, 555−578. (b) Mandal, D. K.; Kishore, N.; Brewer, C. F. *Biochemistry* **1994**, *33*, 1149−1156. (c) Turnbull, W. B.; Stoddart, J. F. *Rev. Mol. Biotech.* **2002**, *90*, 231−255. (d) Lindhorst, T. K. *Top. Curr. Chem.* **2002**, *218*, 201−235.
(13) Pâquet, M. R.; Narasimhan, S.; Schachter, H.; Moscarello, M. A. *J. Biol. Chem.* **1984**, *259*, 4716−4721.
(14) Hennet, T. *Cell. Mol. Life Sci.* **2002**, *59*, 1081−1095.
(15) Rodeheffer, C.; Shur, B. D. *Biochim. Biophys. Acta* **2002**, *1573*, 258−270.
(16) Qasba, P. K.; Ramakrishnan, B.; Boeggeman, E. *Curr. Drug Targets* **2008**, *9*, 292−309.
(17) Ramakrishnan, B.; Balaji, P. V.; Qasba, P. K. *J. Mol. Biol.* **2002**, *318*, 491−502.
(18) Blixt, O.; Norberg, T. *Carbohydr. Res.* **1999**, *319*, 80−91.
(19) Nagahori, N.; Nishimura, S.-I. *Chem.—Eur. J.* **2006**, *12*, 6478−6485.
(20) Laurent, N.; Voglmeir, J.; Flitsch, S. L. *Chem. Commun.* **2008**, 4400−4412.
(21) Houseman, B. T.; Mrksich, M *Angew. Chem, Intl. Ed.* **1999**, *38*, 782−785.
(22) Multivalent enzyme inhibitors exploiting these concepts have been developed. See: (a) Diot, J.; Garcia-Moreno, M. I.; Gouin, S. G.; Ortiz Mellet, C.; Haupt, K.; Kovensky, J. *Org. Biomol. Chem.* **2009**, *7*, 357−363. (b) Compain, P.; Decroocq, C.; Iehl, J.; Holler, M.; Hazelard, D.; Mena Barragan, T.; Ortiz Mellet, C.; Nierengarten, J.-F. *Angew. Chem. Intl. Ed.* **2010**, *49*, 5753−5756.
(23) (a) Gestwicki, J. E.; Cairo, C. W.; Strong, L. E.; Oetjen, K. A.; Kiessling, L. L. *J. Am. Chem. Soc.* **2002**, *124*, 14922−14933. (b) Wilczewski, M.; Van der Heyden, A.; Renaudet, O.; Dumy, P.; Coche-Guerente, L.; Labbe, P. *Org. Biomol. Chem.* **2008**, *6*, 1114−1122. (c) Dam, T. K.; Gerken, T. A.; Brewer, C. F. *Biochemistry* **2009**, *48*, 3822−3827.
(24) Šardzík, R.; Noble, G. T.; Weissenborn, M. J.; Martin, A.; Webb, S. J.; Flitsch, S. L. *Beilstein J. Org. Chem.* **2010**, *6*, 699−703.
(25) Angelova, M. I.; Dimitrov, D. S. *Faraday Discuss. Chem. Soc.* **1986**, *81*, 303−311.
(26) Galla, H. J.; Sackmann, E. *J. Am. Chem. Soc.* **1975**, *97*, 4114−4120.
(27) β4Gal-T1 lost all activity without TX-100, but literature studies indicate a ratio of TX-100:phospholipid below 1:10 should not cause vesicle membrane disruption. More than 10 μM TX-100 was required for dye release from 0.1 μM DPPC vesicles at 50 °C. See: Liu, Y.; Regen, S. L. *J. Am. Chem. Soc.* **1993**, *115*, 708−713.
(28) Metzger, J. W.; Sawyer, W. H.; Wille, B.; Biesert, L.; Bessler, W. G.; Jung, G. *Biochim. Biophys. Acta, Biomembr.* **1993**, *1149*, 29−39.

(29) Shibata, A.; Murata, S.; Ueno, S.; Liu, S.; Futaki, S.; Baba, Y. *Biochim. Biophys. Acta* **2003**, *1616*, 147−155.
(30) Ramakrishnan, B.; Boeggeman, E.; Qasba, P. K. *Biochemistry* **2005**, *44*, 3202−3210.
(31) Christner, J. E.; Distler, J. J.; Jourdian, G. W. *Arch. Biochem. Biophys.* **1979**, *192*, 548−558.
(32) (a) Bains, G.; Lee, R. T.; Lee, Y. C.; Freire, E. *Biochemistry* **1992**, *31*, 12624−12628. (b) Iglesias, J. L.; Lis, H.; Sharon, N. *Eur. J. Biochem.* **1982**, *123*, 247−252.
(33) The increase in rate with membrane loading suggests that perturbation of the conformation of **1** in the membrane by cholesterol is not a significant factor in increasing the reactivity of **1**. See: Lingwood, D.; Binnington, B.; Rog, T.; Vattulainen, I.; Grzybek, M.; Coskun, U.; Lingwood, C. A.; Simons, K. *Nat. Chem. Biol.* **2011**, *7*, 260−262.
(34) Solid supported systems often have more enzyme than immobilized substrate, see: Gutiérrez, O. A.; Chavez, M.; Lissi, E. *Anal. Chem.* **2004**, *76*, 2664−2668.
(35) (a) We found corresponding k_{cat} and K_m values for GlcNAc-PNP with this β4Gal-T1 preparation (HPLC analysis: k_{cat} = 0.1 s^{-1}, K_m = 1 mM) to be at the lower end of literature values for GlcNAc. See references 30, 35b, and 35c. (b) Ramasamy, V.; Ramakrishnan, B.; Boeggeman, E.; Ratner, D. M.; Seeberger, P. H.; Qasba, P. K. *J. Mol. Biol.* **2005**, *353*, 53−67. (c) Ramakrishnan, B.; Boeggeman, E.; Qasba, P. K. *Biochemistry* **2004**, *43*, 12513−12522.
(36) Phospholipids have previously been shown to enhance β4Gal-T1 activity. See: Mitranic, M. M.; Boggs, J. M.; Moscarello, M. A. *J. Biol. Chem.* **1983**, *258*, 8630−8636.
(37) Ohno, K.; Kitano, H. *Bioconj. Chem.* **1998**, *9*, 548−554.
(38) Sheikh, K. H.; Jarvis, S. P. *J. Am. Chem. Soc.* **2011**, *133*, 18296−18303.
(39) Berg, O. G.; Gelb, M. H.; Tsai, M.-D.; Jain, M. K. *Chem. Rev.* **2001**, *101*, 2613−2653.
(40) (a) Honger, T.; Jorgensen, K.; Biltonen, R. L.; Mouritsen, O. G. *Biochemistry.* **1996**, *35*, 9003−9006. (b) Op den Kamp, J. A. F.; De Gier, J.; Van Deenen, L. L. M. *Biochim. Biophys. Acta* **1974**, *345*, 253−256. (c) Mouritsen, O. G.; Andresen, T. L.; Halperin, A.; Hansen, P. L.; Jakobsen, A. F.; Jensen, U. B.; Jensen, M. O.; Joergensen, K.; Kaasgaard, T.; Leidy, C.; Simonsen, A. C.; Peters, G. H.; Weiss, M. *J. Phys.: Condens. Matter* **2006**, *18*, S1293−S1304.
(41) Jain, M. K.; Berg, O. G. *Biochim. Biophys. Acta* **1989**, *1002*, 127−156.
(42) (a) Šardzík, R.; Sharma, R.; Kaloo, S.; Voglmeir, J.; Crocker, P. R.; Flitsch, S. L. *Chem. Commun.* **2011**, *47*, 5425−5427. (b) Noble, G. T.; Craven, F.; Šardzík, R.; Flitsch, S. L.; Webb, S. J. Unpublished results.
(43) Ats, S.-C.; Lehmann, J.; Petry, S. *Carbohydr. Res.* **1994**, *252*, 325−332.
(44) Wild-type β4Gal-T1 is membrane-bound *in vivo* and acts within this two-dimensional matrix rather than three-dimensions available to the soluble version used here. However the same general principles should hold, although the enhancement in apparent K_m may not be as great and may be affected by additional steric barriers.
(45) Qasba, P. K.; Ramakrishnan, B.; Boeggeman, E. *Trends Biochem. Sci.* **2005**, *30*, 53−62.
(46) (a) Levengood, M. R.; Splain, R. A.; Kiessling, L. L. *J. Am. Chem. Soc.* **2011**, *133*, 12758−12766. (b) May, J. F.; Splain, R. A.; Brotschi, C.; Kiessling, L. L. *Proc. Natl Acad. Sci. U.S.A.* **2009**, *106*, 11851−11856. (c) Perlstein, D. L.; Wang, T.-S. A.; Doud, E. H.; Kahne, D.; Walker, S. *J. Am. Chem. Soc.* **2010**, *132*, 48−49.
(47) Leser, G. P.; Lamb, R. A. *Virology* **2005**, *342*, 215−227.